



Lamb–Dicke localization of cold atoms in Ferris wheel optical dipole potential

V. E. LEMBESSIS,*  A. LYRAS, AND O. M. ALDOSSARY 

Quantum Technology Group, Department of Physics and Astronomy, College of Science, King Saud University, Riyadh 11451, Saudi Arabia
*Corresponding author: vlembessis@gmail.com

Received 22 September 2021; revised 1 November 2021; accepted 1 November 2021; posted 1 November 2021;
published 24 November 2021

We investigate the possibility of strong localization, of the Lamb–Dicke type, for cold atoms trapped by a far off-resonant Ferris wheel optical dipole potential. This optical dipole potential light field is created when a light field generated by the superposition of two similar co-propagating Laguerre–Gaussian beams, with opposite winding numbers, interacts with a two-level atom. We show that strong confinement of atoms in such a light field is possible when the light field is tightly focused, for low values of the winding number and relatively high values of power. We show that a combination of a Ferris wheel with an ordinary axial Gaussian optical lattice provides 3D cylindrically symmetric optical lattices in which the Lamb–Dicke limit can be reached for typically used experimental parameter values. © 2021 Optica Publishing Group

<https://doi.org/10.1364/JOSAB.443903>

1. INTRODUCTION

The advent of optical vortex beams has given a significant boost to the research of mechanical effects of light on atoms, namely, optical cooling and trapping. Optical vortices are coherent beams made up by photons that are endowed with a quantized orbital angular momentum (OAM), along the beam propagation axis. The magnitude of this OAM is given by $\ell\hbar$, where ℓ is a nonzero integer number known as the winding number of the beam [1]. Due to this OAM of the photons, the beam exchanges orbital angular momentum with the atoms in addition to the exchange of linear momentum. Moreover, optical vortices, known also as twisted beams, have a rich spatial structure both in their phase and amplitude, which offers new opportunities for atom manipulation. The so-called Laguerre–Gaussian (LG) beams and Bessel beams are the most popular members of this class of laser beams. Photon OAM, together with the highly structured character of the intensity profile of these beams, is responsible for the novel mechanical effects of optical vortices on atoms [2].

When we interfere two co-propagating LG beams with opposite winding numbers (i.e., $\ell_1 = -\ell_2 = \ell$), we create the so-called optical Ferris wheel [3]. This is a coherent light field characterized by a petal-like intensity structure at the transverse plane made up by 2ℓ bright regions. This field supports 2D cylindrically symmetric optical lattices, which have been shown to offer new opportunities for atomic conveyors and realizations of cold atom collisional quantum gates [4]. If the two beams are counterpropagating, we obtain helical optical tubes that can serve as Archimedes' spiral for atoms [5,6], which can be applied in quantum metrology and rotational sensing [7] and

in the realization of quantum collisional gates [4]. The idea of an optical Ferris wheel has been transferred to atom beams with the proposal of an atomic Ferris wheel [8].

When we attempt Doppler-free spectroscopy with trapped atoms, the key point is to achieve a suppression of the recoil, which accompanies the absorption/emission of a photon by the atom. Such a suppression is possible whenever a particle is confined in a region of space. The story started in 1939 when Lamb did calculations on the absorption of neutrons by the nucleus of an atom bound in a crystalline lattice [9]. The calculations showed a narrow recoil-free component in the absorption rate of neutrons when the binding is very strong. In 1953, Dicke considered a radiating atom trapped in a 1D well and oscillating back and forth between the walls of the well [10]. Dicke noticed that, in the case where the atom is deeply confined in the well, the Doppler shift, associated with the motion of the atom in the well, does not modulate the frequency of the emitted radiation. To honor their pioneering work, the strong confinement of a particle is known as the Lamb–Dicke limit. This work drove atomic physicists to consider the extension of these ideas to the optical domain of the spectrum. To do so, they had to find ways to localize atoms in small regions of space. In 1968, Letokhov first realized that this would be possible if the atoms were localized in the nodes or antinodes of standing laser waves [11]. In the next decades, the experimental progress in laser cooling and trapping techniques made all these possible. In 1990, Westbrook *et al.* observed Lamb–Dicke narrowing in the resonance fluorescence of Na atoms trapped in three dimensions [12]. Two years later, the localization of Rb atoms in a 1D potential well was observed [13]. In those

experimental works, the atoms were trapped in an optical molasses configuration. In 1997, the Lamb–Dicke narrowing was observed in a far-detuned 1D optical trap filled with Cs atoms [14].

Optical dipole traps enabled the opportunity of deep trapping of the cooled atomic particles ending up to strong localization of them where the uncertainty on the atomic particle's position is much smaller compared with the wavelength of the light ($\Delta x \ll \lambda$). In such a case, the recoil energy is far smaller than the spacing between the vibrational levels of the trapping potential. Thus, the atom after any spontaneous/stimulated emission absorption cycle returns back to the vibration level where it started from. Due to this suppression of the recoil effect, when combined with the low heating rates in a far-detuned optical dipole trap, this case offers an ideal environment for high-resolution spectroscopy, for sideband-resolved Raman cooling, and the creation and study of nonclassic states of the atomic gross motion [14]. Optical dipole trapping in optical lattices has been shown to work as an efficient mechanism for reaching the Lamb–Dicke limit. Westbrook *et al.* used a configuration of two couples (one at $x - z$ plane and the other at $y - z$) of counterpropagating beams, at an angle, to create a 3D optical lattice and showed that they could reach the Lamb–Dicke limit for an atom trapped inside the lattice. By changing the lattice angle, the size of the potential wells changes, and, with this method, they varied the value of the Lamb–Dicke parameter [15]. In 1998, Friebe *et al.* managed to realize a 1D optical lattice for Rb atoms created by a CO₂ laser operating at 10.6 μm , where the trapping sites had a period of 5.3 μm , almost seven times longer than the wavelength of the Rb D2 line [16]. In 2000, Scheunemann *et al.* showed that such a lattice can be used to reach the Lamb–Dicke limit for a trapped Rb atom in a far detuned 1D optical lattice [17]. Because of the large detuning, in optical dipole trapping with a CO₂ laser, the atomic polarizability is approximately equal to its static value, which is positive for the ground and excited states. Thus, in this case, the trapping is not similar to that in conventional dipole traps; for whatever the internal atomic state is, the atom will be confined by the potential. Such type of trapping has a unique combination of properties, e.g., the low spontaneous scattering rate, the long storage time, and quite steep potential wells. Further, its spatial period is far larger than the conventional near-resonant optical lattices, so it allows spatial resolution of the fluorescence signal emitted by the atoms in each individual trapping site. This property makes it an ideal environment for direct study of tunneling, diffusion, and transport of atoms between lattice sites [16] and for atom cooling at its ground state with the help of sideband cooling [18]. It is also of great importance in the operation of optical lattice atomic clocks [19].

In this work, we investigate the possibility of reaching strong confinement and the Lamb–Dicke limit when a cold Cs atom is optically dipole trapped at the focus of a far detuned Ferris wheel light field. The structure of the paper is as follows. In Section 2, we briefly present the optical dipole potential in a Ferris wheel light field. In Section 3, we show, by using numerical examples, based on parameter values that are typically used in cold atom experiments, how we can reach the Lamb–Dicke limit in an optical Ferris wheel. Our calculations show that this is an ideal environment for reaching the Lamb–Dicke limit in two dimensions (on the transverse plane); however, the weak axial trapping

restricts the efficiency of the Ferris wheel for reaching the Lamb–Dicke limit in three dimensions. In Section 4, we show how we can overcome this problem by combining the Ferris wheel with an ordinary axial Gaussian optical lattice forming a 3D lattice with cylindrical symmetry.

2. PHYSICS OF THE PROBLEM

The intensity of the electric field of a Ferris wheel light field of wavelength λ , linearly polarized along the x direction, and propagating along the z direction, with a power P , is given by

$$I(\mathbf{R}) = I_0 u_{p,|\ell|}(\mathbf{R}), \quad (1)$$

where

$$u_{p,|\ell|}(\mathbf{R}) = \frac{C_{p,|\ell|}}{\sqrt{1 + z^2/z_R^2}} \left(\frac{\rho\sqrt{2}}{w(z)} \right)^{|\ell|} \times \exp\left(-\frac{2\rho^2}{w_0^2}\right) L_p^{|\ell|} \left(\frac{2\rho^2}{w^2(z)} \right) \cos(\ell\phi), \quad (2)$$

while $I_0 = P/(\pi w_0^2)$.

The quantity w_0 is the beam waist, $z_R = \pi w_0^2/\lambda$ is the Rayleigh range of the beam, $w(z) = w_0\sqrt{1 + z^2/z_R^2}$, $C_{p,|\ell|} = \sqrt{2p!/\pi(|\ell| + p)!}$, and $L_p^{|\ell|}(\frac{2\rho^2}{w_0^2})$ the corresponding associated Laguerre polynomial.

The optical dipole trapping of a two-level prototype atomic system of transition frequency ω_0 , irradiated by a Ferris wheel beam, has been presented analytically in [4]. However, in the case of very large detuning, as in the case of irradiation by a CO₂ laser, we approach the regime of the so-called quasi electrostatic trapping [20,21]. In this case, the optical dipole potential is given by [22]

$$U = -\frac{3\pi c^2}{\omega_0^3} \frac{\Gamma}{\omega_0} I(\mathbf{R}). \quad (3)$$

Figure 1 presents the plot of the potential on the $x - y$ plane for $\ell = 2$. When the detuning is negative (red), the atoms can be trapped in the bright (high-intensity) regions. For deep atom trapping, we consider the simple harmonic approximation around a minimum of the optical dipole potential. In the trapping region located on the positive x axis, as shown in Fig. 1, and for red detuning, the potential has a minimum at $(x_0, y_0, z_0) = (w_0\sqrt{|\ell|/2}, 0, 0)$. By performing a Taylor expansion around this minimum, we find the following approximation for the trapping potential:

$$U(x, y, z) = U_0 - \frac{1}{2}k_x \left(x - w_0\sqrt{\frac{|\ell|}{2}} \right)^2 - \frac{1}{2}k_y y^2 - \frac{1}{2}k_z z^2, \quad (4)$$

where the spring constants k_x , k_y , k_z , and U_0 are given by

$$k_x = \frac{16A|\ell|^{|\ell|}e^{-|\ell|}}{\pi w_0^2|\ell|!}, \quad k_y = \frac{8A|\ell|^{|\ell|}e^{-|\ell|}}{\pi w_0^2(|\ell| - 1)!},$$

$$k_z = \frac{2A|\ell|^{|\ell|}e^{-|\ell|}}{\pi z_R^2|\ell|!}, \quad U_0 = \frac{2A|\ell|^{|\ell|}e^{-|\ell|}}{\pi|\ell|!}, \quad (5)$$

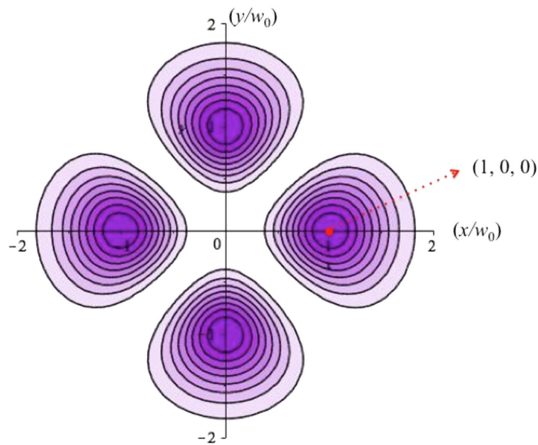


Fig. 1. Transverse profile ($z = 0$) of the trapping potential for a Ferris light field with $|\ell| = 2$. The coordinates of the deepest trapping position on the x axis are given.

where

$$A = \frac{3\pi c^2 \Gamma}{\omega_0^3 \omega_0} I_0. \quad (6)$$

The eigenfunctions of the trapped atoms are, accordingly [4],

$$\begin{aligned} \Psi_{m,s,p} = & \left(\frac{\xi_x \xi_y \xi_z}{\pi^3} \right)^{1/2} \frac{1}{\sqrt{2^{m+s+p} m! s! p!}} \\ & \times H_m \left(\xi_x \left(x - w_0 \sqrt{\frac{|\ell|}{2}} \right) \right) H_s(\xi_y y) H_p(\xi_z z) \\ & \times \exp \left\{ - \frac{\left[\xi_x \left(x - w_0 \sqrt{\frac{|\ell|}{2}} \right) \right]^2 + (\xi_y y)^2 + (\xi_z z)^2}{2} \right\}, \end{aligned} \quad (7)$$

where $H_{m,s,p}$ are Hermitian polynomials, $\xi_{x,y,z} = \sqrt{\left(\frac{M\omega_{x,y,z}}{\pi\hbar} \right)}$, $\omega_{x,y,z} = \sqrt{k_{x,y,z}/M}$, M is the mass of the atom, and $m, s, p = 0, 1, 2, \dots$ are positive integers. The rms of the atomic position along the three directions is given by $\Delta x = (\pi\hbar/M\omega_x)^{1/2}$, $\Delta y = (\pi\hbar/M\omega_y)^{1/2}$, and $\Delta z = (\pi\hbar/M\omega_z)^{1/2}$, which, if we take into account the expression in Eq. (6), are given (in units of the optical vortex wavelength) by the relations

$$\begin{aligned} \Delta x = \sqrt{\pi\hbar} \left\{ \frac{1}{Mk_x} \right\}^{1/4}, \quad \Delta y = \sqrt{\pi\hbar} \left\{ \frac{1}{Mk_y} \right\}^{1/4}, \\ \Delta z = \sqrt{\pi\hbar} \left\{ \frac{1}{Mk_z} \right\}^{1/4}, \end{aligned} \quad (8)$$

where $k_{x,y,z}$ are given in Eq. (5).

3. LAMB-DICKE LOCALIZATION

The relations in Eq. (8) for the rms of the atomic position are adequate to show us when we can reach the Lamb–Dicke limit.

Normally in theoretical and experimental work, it is sufficient for these quantities to be smaller than 0.1λ . We are going to consider, as in [16], that our Ferris wheel lattice is created by a CO₂ laser operating at $\lambda = 10.6 \mu\text{m}$ interacting with a Cs atom at the $6^2S_{1/2}$ to $6^2S_{3/2}$ transition at $\lambda_0 = 852.35 \text{ nm}$. This ensures far detuned optical dipole trapping with a detuning $\Delta = 2 \times 10^{15} \text{ Hz}$. The reason we choose the Cs atom is that it is the heaviest atom employed in trapping experiments, thus ensuring better localization. The mass of the Cs atom is $M = 2.2 \times 10^{-25} \text{ kg}$. In the experiment in [16], the authors used beams with a beam waist of 3.3λ ($35 \mu\text{m}$) and a power of 14 W ; they commented, however, that higher powers and smaller beam waists could give them even better results in their attempt to reach the Lamb–Dicke limit. In our following numerical work, we consider a maximum power up to 100 W and a beam waist varying from 0.5λ ($5.3 \mu\text{m}$) up to 3λ ($31.8 \mu\text{m}$). In Fig. 2, we present the plots for the three rms quantities in Eq. (8) in units of CO₂ laser wavelength as functions of the beam waist and the value of available power. We consider for our Ferris that $\ell = 1$.

As we can see from the plots, as the power increases and beam waist decreases, we can reach the Lamb–Dicke limit. Our numerical calculations have shown that this tendency is preserved if we increase the winding number values up to $\ell = 4$ for the same range of power values. However, as the winding number is increased, the potential at trapping sites becomes shallower, and the Lamb–Dicke limit cannot be approached in the z direction, although, in the transverse direction, we remain in the Lamb–Dicke limit for much higher values of the winding number (higher than $\ell = 600$). Similar is the situation if we consider the relative size of the beam waist. In the longitudinal direction, we cannot reach the limit for beam waists larger than 3λ , while we can stay within this limit in the transverse direction for beam waists up to 11λ .

In our example above, since $\ell = 1$, the Ferris wheel has two trapping sites located at the points $(x_0, y_0, z_0) = (\pm w_0 \sqrt{1/2}, 0, 0)$, which means that the distance between the two trapping sites is $w_0 \sqrt{2}$. In the case where $w_0 = 3\lambda$, the relative distance is $45 \mu\text{m}$ or $52.8\lambda_0$. As shown, the relative spacing is far larger than the resonant wavelength λ_0 , which makes our scheme a good candidate for investigations in the spatial domain. This spacing decreases as we increase the value of the winding number because we create more trapping sites on the transverse plane. In the general case, two adjacent trapping sites have a relative distance equal to $w_0 \sqrt{2}/|\ell|$. When we use a 1D lattice as in [17], the relative distance is $\lambda/2$. This means that our scheme could provide larger spacing (in the transverse plane) for $|\ell| < 2\sqrt{2}w_0/\lambda$ or $|\ell| \leq 8$.

In such experiments, the values of the trapping frequencies, the photon scattering rate that determines the lifetime of the trapping scheme, and the energy depth of the trap are of particular importance. In Fig. 3, we present the trapping frequencies (in kHz) that correspond to the parameters of Fig. 1. In Fig. 4, we present the photon scattering rate (in kHz) and the trap depth (in mK), which corresponds to the parameters shown in Fig. 1.

By carefully examining Figs. 1–3 and for a beam waist $w_0 = 3\lambda$ and a power of 200 W , which is the lowest one for which the Lamb–Dicke is ensured in three dimensions, we

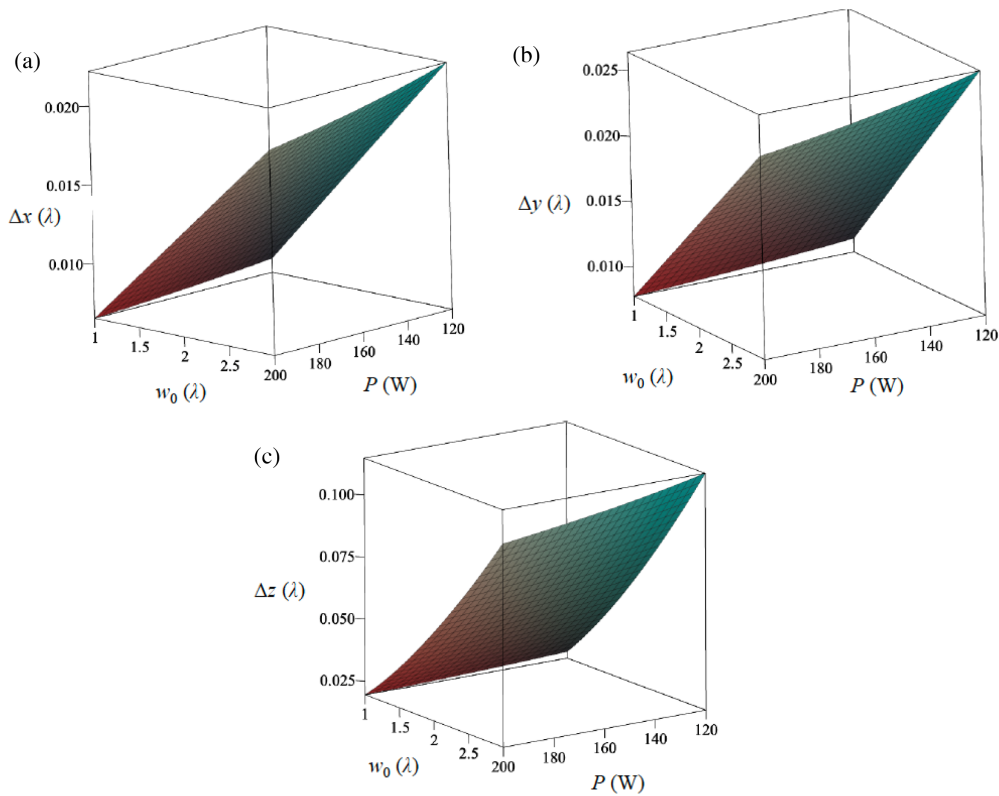


Fig. 2. The rms position, in the (a) x direction, (b) y direction, and (c) z direction, of a trapped Cs atom in a Ferris light field ($\ell = 1$) of wavelength $\lambda = 10.6 \mu\text{m}$ as a function of power and beam waist. The rms position and beam waist are scaled in wavelength units. All the quantities have been calculated at $z = 0$.

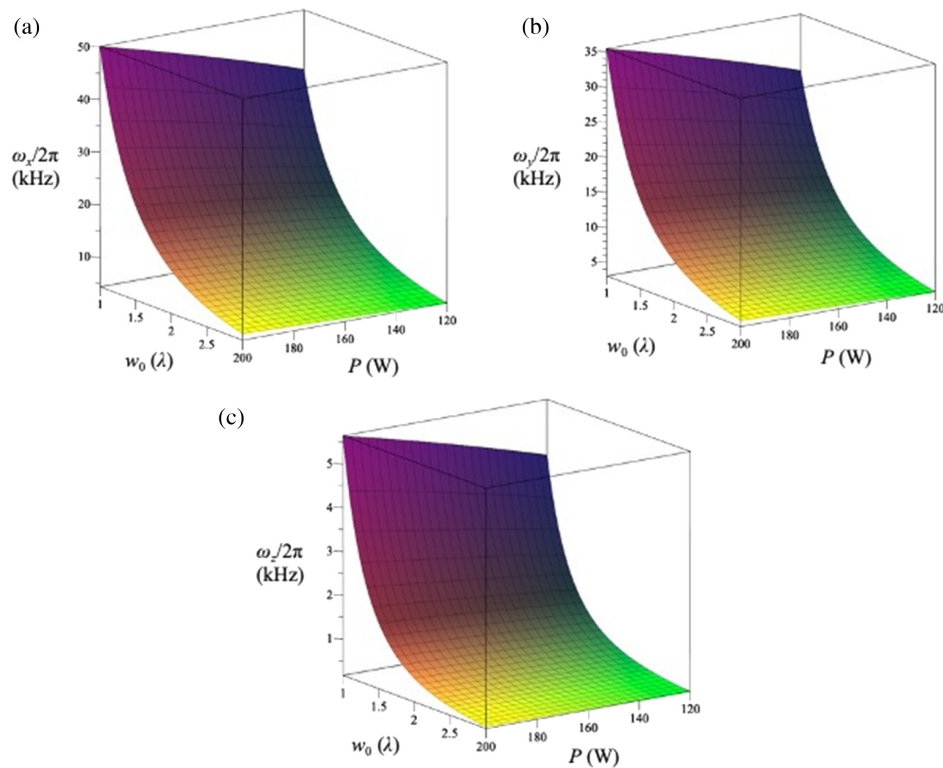


Fig. 3. Oscillation angular frequencies, in the (a) x direction, (b) y direction, and (c) z direction, of a trapped Cs atom in a Ferris light field ($\ell = 1$) of wavelength $\lambda = 10.6 \mu\text{m}$ as a function of the power of one beam and beam waist. The beam waists are scaled in wavelength units. All the quantities have been calculated at $z = 0$.

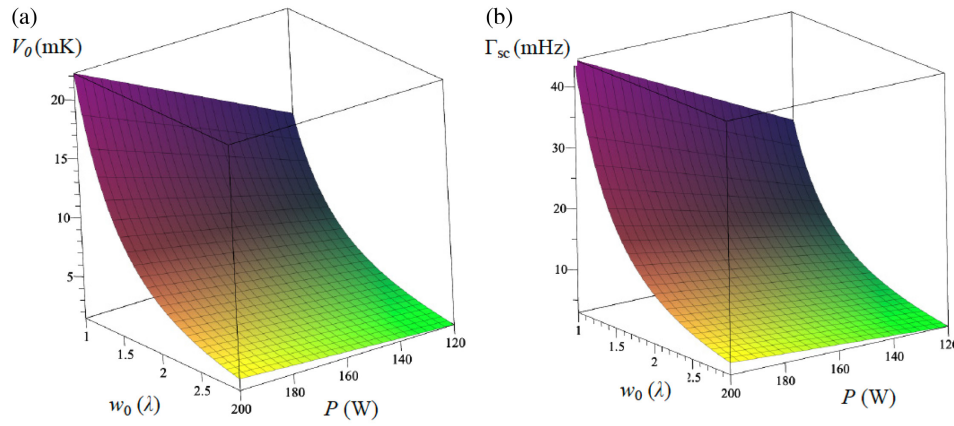


Fig. 4. (a) Potential depth and (b) the photon scattering rate of a trapped Cs atom in a Ferris light field ($\ell = 1$) of wavelength $\lambda = 10.6 \mu\text{m}$ as a function of power of one beam and beam waist. The beam waists are scaled in wavelength units. All the quantities have been calculated at $z = 0$.

obtain the following values for the trapping angular frequencies, scattering rate, and potential depth: $\omega_x/2\pi = 6 \text{ kHz}$, $\omega_y/2\pi = 4.2 \text{ kHz}$, $\omega_z/2\pi = 0.23 \text{ kHz}$, $\Gamma_{\text{sc}} = 5.5 \text{ mHz}$, and $V_0 = 2.6 \text{ mK}$. In the experiment in [17] with a power of 14 W and a beam waist of 3.5λ , the authors achieved a radial ($x - y$ plane) frequency $\omega_{x,y}/2\pi = 5.7 \text{ kHz}$, an axial (z direction) frequency $\omega_z/2\pi = 59 \text{ kHz}$, and a potential depth $V_0 = 2.1 \text{ mK}$, while $\Gamma_{\text{sc}} = 5 \text{ mHz}$. We clearly see that our scheme is more power demanding, as it is expected for any scheme that uses LG beams. The scattering rate presented in Fig. 4 is given by the relation $\Gamma_{\text{sc}} = 2\Gamma V_0 \omega^3 / \hbar \Delta \omega_0^4$, where in our case $\Gamma/2\pi = 5.18 \text{ MHz}$ [22]. However, we must point out that, for an atom trapped in the ground state in the Lamb–Dicke limit, the actual photon scattering rate is suppressed to a value Γ'_{sc} smaller than Γ_{sc} by the factor $(k\xi)^2$ where $\xi = \sqrt{(\Delta x)^2 + (\Delta y)^2 + (\Delta z)^2}$ [23].

Before we finish this section, we would like to comment on another interesting issue. When an atom is confined in a trap and rests at a certain vibrational level described by a wavefunction $|\Psi_{m,s,p}\rangle$, the emission or absorption of a photon may cause a transition to another vibrational level $|\Psi_{m',s',p'}\rangle$. The intensity I of this transition is simply proportional to the square modulus of the matrix element involving the external degrees of freedom [19]:

$$I = |\langle \Psi_{m,s,p} | u_{p,|\ell|}(\mathbf{R}) \exp(i\Theta_{p,|\ell|}(\mathbf{R})) | \Psi_{m',s',p'} \rangle|^2. \quad (9)$$

When an atom is strongly localized in the trap, its interaction with the light field could have two results. Either it leaves the atom at the ground state of the trap or raises it on higher excited states, mainly to the first excited state. In general, the calculation of I can be done only numerically. However, if the atom is well localized, we can calculate I analytically for the case where $(m, s, p) = (0, 0, 0)$, while $(m', s', p') = (0, 0, 0)$. The reason is that, when the atom is in the Lamb–Dicke localization regime, then the Gaussian functions of the ground quantum SHO eigenstates can be approximated by delta functions, thus

$$\begin{aligned} I_{000 \rightarrow 000} &= |\langle \Psi_{0,0,0} | u_{p,|\ell|}(\mathbf{R}) \exp(i\Theta_{p,|\ell|}(\mathbf{R})) | \Psi_{0,0,0} \rangle|^2 \\ &= |u_{p,|\ell|}(\mathbf{R}_0) \exp(i\Theta_{p,|\ell|}(\mathbf{R}_0))|^2, \end{aligned} \quad (10)$$

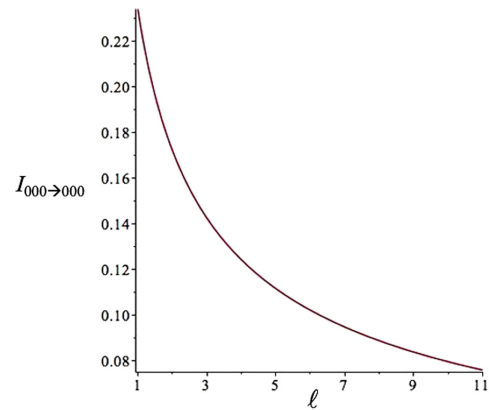


Fig. 5. Value of the transition matrix element $I_{000 \rightarrow 000}$ as a function of $|\ell|$ in the case of strong confinement.

where $\mathbf{R}_0 = (w_0 \sqrt{|\ell|}/2, 0, 0)$. In this case, $\exp(i\Theta_{p,|\ell|}(\mathbf{R}_0)) = 1$ and thus $I_{000 \rightarrow 000} = |u_{p,|\ell|}(\mathbf{R}_0)|^2$. If the experimental conditions ensure a strong localization, then at this limit the matrix elements $I_{000 \rightarrow 100}$, $I_{000 \rightarrow 010}$, and $I_{000 \rightarrow 001}$ are equal to zero. We may have an analytical form for the matrix element $I_{000 \rightarrow 000}$ in this case given by (in the case, where $p = 0$):

$$I_{000 \rightarrow 000} = |u_{p,|\ell|}(\mathbf{R}_0)|^2 = \frac{2}{\pi |\ell|!} |\ell|^{|\ell|} \exp(-2|\ell|). \quad (11)$$

An interesting feature of this formula is that the value of this quantity does not depend on the beam waist size (as far as strong localization assumption is considered); Fig. 5 shows it is reduced as the winding number increases. The reason for this behavior is that, when the atom is so strongly localized and its wavefunction can be approximated by a delta function, the width of the beam represented by the relevant size of the beam waist w_0 does not affect its state in the trap. The decrease of the quantity $I_{000 \rightarrow 000}$, as the winding number increases, is due to the fact that, for given power, the trapping sites get shallower with higher $|\ell|$.

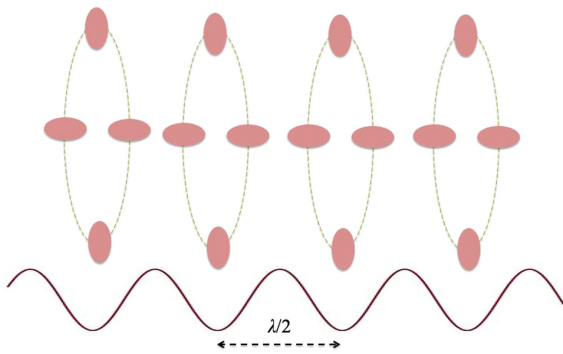


Fig. 6. Addition of a Gaussian standing wave along the z direction leads to a stack of Ferris wheel trapping sites.

4. TOWARD A ROBUST 3D LAMB-DICKE LOCALIZATION

In this section, we propose a robust 3D Lamb–Dicke localization by combining the benefits of trapping in conventional axial lattice, which gives tight axial trapping, and of a Ferris lattice, which gives tight transverse trapping. For this, we add another 1D Gaussian optical lattice along the z direction of the same wavelength to make trapping deeper, as we have proposed in our collisional gates paper [4] and as shown in Fig. 6.

The new lattice is characterized by a beam waist that is three times larger than the Ferris wheel beam waist. The reason is that we need the Gaussian lattice to have a considerable off-axis intensity since on the transverse plane the Ferris wheel lattice has its maximum intensity on a ring. We also consider that

each beam in the two lattices has power P . The Ferris wheel is characterized by a winding number $|\ell| = 5$, so it has 10 trapping sites. We obtain Figs. 7–9 for the rms of atomic position, the trapping angular frequencies, the potential depth and scattering rate, respectively.

The results in Figs. 7–9 show that, if we combine the two lattices, we can reach easily the Lamb–Dicke limit in three dimensions for reasonable experimental parameter values with less total power. Moreover, in the example considered above, we can accommodate up to 10 atoms on the transverse plane at a distance up to $3.16\lambda = 3.4\ \mu\text{m}$ (when we choose a beam waist equal to 5λ) while along the axial direction the distance between neighboring sites is $\lambda/2 = 5.3\ \mu\text{m}$. The atoms, thus, are at a quite large distance apart from each other, which is an ideal environment for spatially resolved spectroscopy. As these stacks of trapping sites are repeated axially (Fig. 6), we can have a large number of atoms trapped in the Lamb–Dicke limit. However, in this case, there is a decrease of trapping angular frequency ω_z as we move along the axis since the trapping depth decreases both in the Ferris wheel and in the Gaussian axial lattices. All the plots presented in this work are valid at the focus ($z = 0$). We must point out that the trapping potential of the Ferris in the axial direction is enhanced by the trapping potential of the Gaussian lattice, while the trapping properties in the transverse plane are not significantly affected. At the equilibrium position, we have made a simple harmonic approximation of the total potential and from it we obtain the rms value for Δz , Δy , and Δx and the values for $\omega_{x,y,z}$ which we show in the plots. The presence of the Gaussian lattice leads to a slight increase in the values of Δy and Δx and a slight decrease in the values of $\omega_{x,y}$. These changes

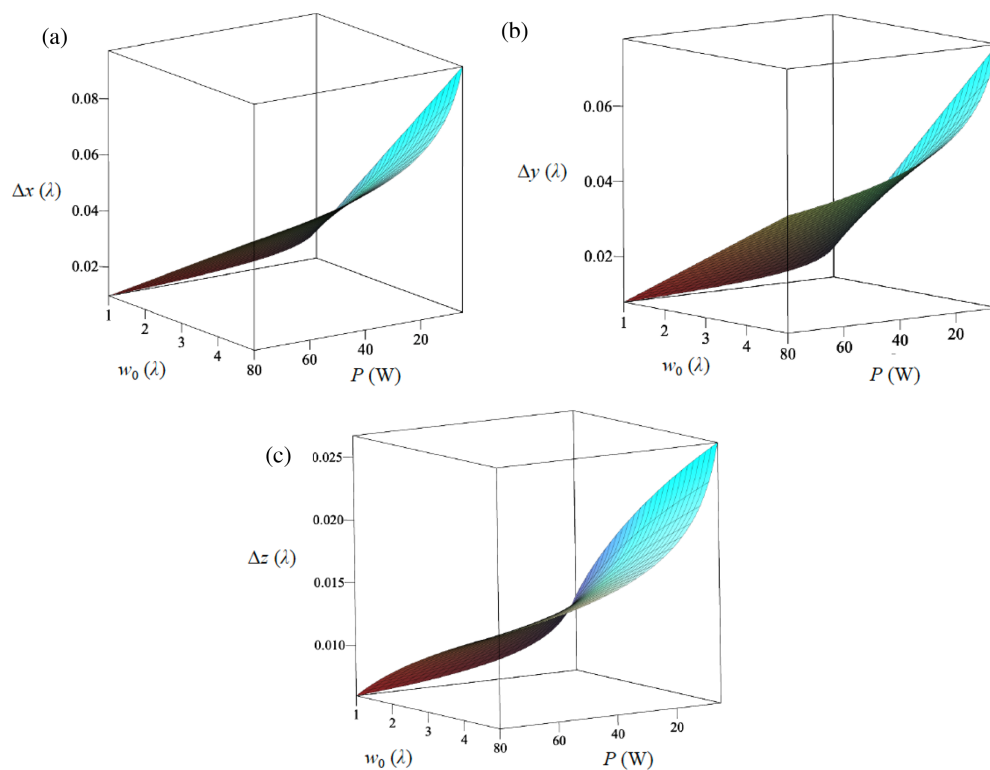


Fig. 7. The rms position, in the (a) x direction, (b) y direction, and (c) z direction, of a trapped Cs atom in a Ferris light field ($\ell = 5$) of wavelength $\lambda = 10.6\ \mu\text{m}$, combined with an axial Gaussian lattice with a three times larger beam waist, as a function of the power of each beam and the Ferris beam waist. The beam waists are scaled in wavelength units. All the quantities have been calculated at $z = 0$.

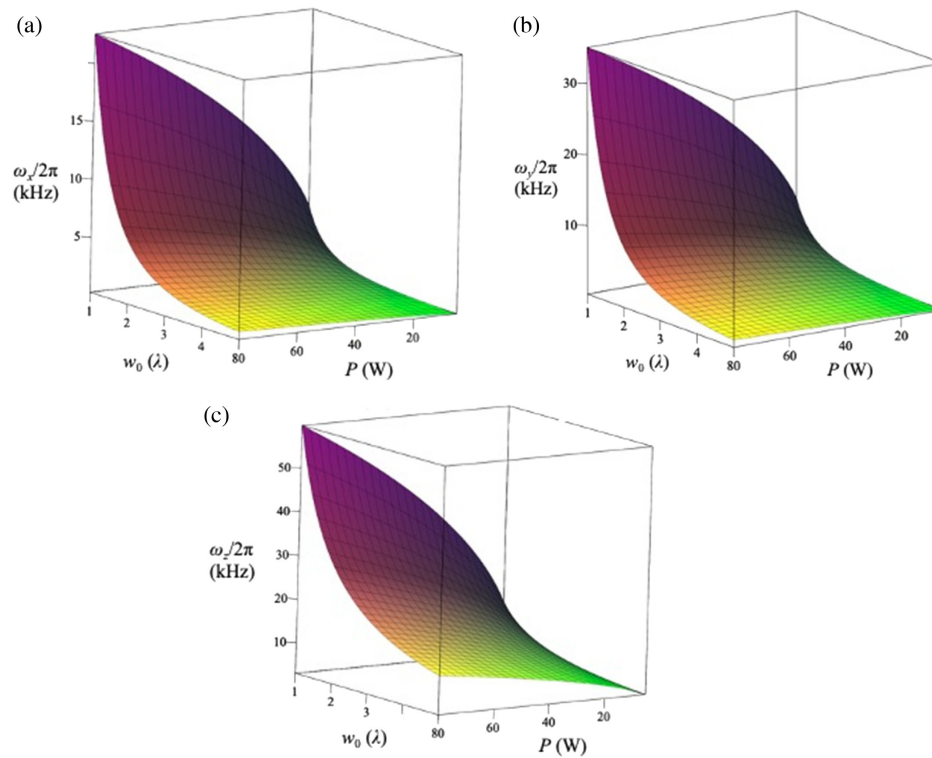


Fig. 8. Oscillation angular frequencies, in the (a) x direction, (b) y direction, and (c) z direction, of a trapped Cs atom in a Ferris light field ($\ell = 5$) of wavelength $\lambda = 10.6 \mu\text{m}$, combined with an axial Gaussian lattice with a three times larger beam waist, as a function of the power of each beam and the Ferris beam waist. The beam waists are scaled in wavelength units. All the quantities have been calculated at $z = 0$.

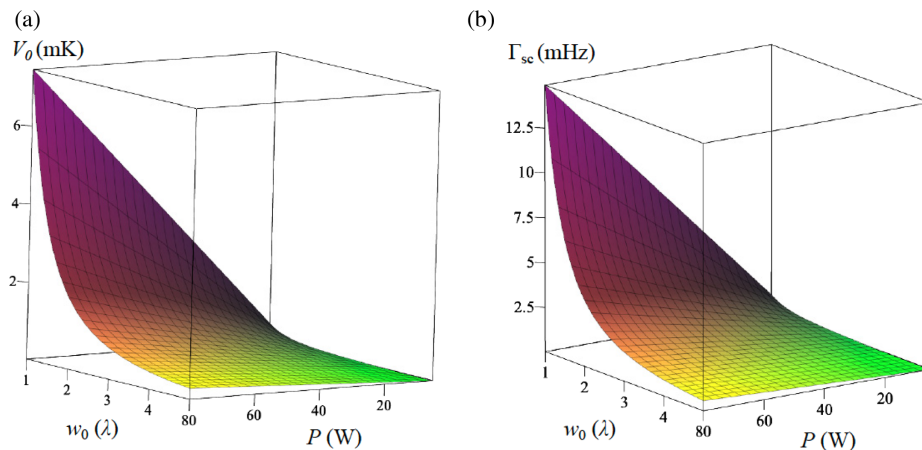


Fig. 9. (a) Potential depth and (b) the photon scattering rate of a trapped Cs atom in a Ferris light field ($\ell = 5$) of wavelength $\lambda = 10.6 \mu\text{m}$, combined with an axial Gaussian lattice with a three times larger beam waist, as a function of the power of each beam and Ferris beam waist. The beam waists are scaled in wavelength units. All the quantities have been calculated at $z = 0$.

reflect the fact that the addition of the Gaussian lattice makes the trapping sites on the transverse plane shallower.

5. CONCLUSIONS

In this paper, we have investigated the possibility of approaching the Lamb–Dicke limit when an atom is confined by the optical dipole potential in a far-detuned Ferris wheel coherent light field. Our theoretical and numerical analysis showed that such a scenario is possible only in cases where the Ferris wheel field

is created by the interference of LG beams with low winding numbers, for given power. The reason is that, even under tight focusing conditions, the trapping in the axial direction is weaker compared with that on the transverse plane. So, in the event of a photon absorption/emission, the atom is highly likely to leave the ground state of the trapping potential and jump to a higher excited one. The optical Ferris wheel could be used as an alternative trapping scheme for approaching the Lamb–Dicke limit. However, it is more power-consuming. A lattice with cylindrical symmetry could be created by a combination of a Ferris wheel

with an ordinary axial Gaussian optical lattice. Such a lattice offers a large number of trapping sites both in the transverse and along the axial direction where we can reach the Lamb–Dicke limit. We must point out that this scheme requires four beams, while for ordinary Gaussian lattices we need six beams to realize a 3D lattice. We must emphasize that the number of trapping sites, on the transverse plane, can be further increased if we use LG beams with a nonzero radial index p . This is so because the transverse intensity profile of LG beams has $p + 1$ bright rings. However, this scheme would require much more power, as the intensity and thus the trap depth in the outer rings will be smaller. Experimental work on such types of lattices still lags behind the theoretical work; however, we believe that they provide a novel trapping landscape for cold atoms, i.e., a novel type of optical lattice where much of exotic physics is anticipated.

Funding. King Abdulaziz City for Science and Technology (15-MAT5110-02).

Acknowledgment. This project was funded by the National Plan for Science, Technology and Innovation (MAARIFAH), King Abdulaziz City for Science and Technology, Kingdom of Saudi Arabia, Award Number (15-MAT5110-02).

Disclosures. The authors declare no conflicts of interest.

Data Availability. Data underlying the results presented in this paper are not publicly available at this time but may be obtained from the authors upon reasonable request.

REFERENCES

1. L. Allen, M. W. Beijersbergen, R. J. C. Spreeuw, and J. P. Woerdman, "Orbital angular momentum of light and the transformation of Laguerre-Gaussian laser modes," *Phys. Rev. A* **45**, 8185–8189 (1992).
2. M. Babiker, D. L. Andrews, and V. E. Lembessis, "Atoms in complex twisted light," *J. Opt.* **21**, 013001 (2018).
3. S. Franke-Arnold, J. Leach, M. J. Padgett, V. E. Lembessis, D. Ellinas, A. J. Wright, J. M. Girkin, P. Ohberg, and A. S. Arnold, "Optical Ferris wheel for ultracold atoms," *Opt. Express* **15**, 8619–8625 (2007).
4. V. E. Lembessis, A. Lyras, and O. M. Aldossary, "Optical Ferris wheels as a platform for collisional quantum gates," *J. Opt. Soc. Am. B* **38**, 233–240 (2021).
5. A. Al Rsheed, A. Lyras, V. E. Lembessis, and O. M. Aldossary, "Guiding of atoms in helical optical potential structures," *J. Phys. B* **49**, 125002 (2016).
6. A. Al Rsheed, A. Lyras, O. Aldossary, and V. E. Lembessis, "Rotating optical tubes for vertical transport of atoms," *Phys. Rev. A* **94**, 063423 (2016).
7. A. Y. Okulov, "Superfluid rotation sensor with helical laser trap," *J. Low Temp. Phys.* **171**, 397–407 (2013).
8. V. E. Lembessis, "Atomic Ferris wheel beams," *Phys. Rev. A* **96**, 013622 (2017).
9. W. E. Lamb, "Capture of neutrons by atoms in a crystal," *Phys. Rev.* **55**, 190–197 (1939).
10. R. H. Dicke, "The effect of collisions upon the Doppler width of spectral lines," *Phys. Rev.* **89**, 472–473 (1953).
11. V. S. Letokhov, "Narrowing of the Doppler width in a standing light wave," *J. Theor. Exp. Phys. Lett.* **7**, 272–275 (1968).
12. C. I. Westbrook, R. N. Watts, C. E. Tanner, S. L. Rolston, W. D. Phillips, and P. D. Lett, "Localization of atoms in a three-dimensional standing wave," *Phys. Rev. Lett.* **65**, 33–36 (1990).
13. P. S. Jessen, C. Gerz, P. D. Lett, W. D. Phillips, S. L. Rolston, R. J. C. Spreeuw, and C. I. Westbrook, "Observation of quantized motion of Rb atoms in an optical field," *Phys. Rev. Lett.* **69**, 49–52 (1992).
14. D. L. Haycock, S. E. Hamann, G. Kiose, and P. S. Jessen, "Atom trapping in the Lamb-Dicke regime in a far-off-resonance optical lattice," *Proc. SPIE* **2995**, 163–172 (1997).
15. C. I. Westbrook, C. Jurczak, G. Birkly, B. Desruelle, W. D. Phillips, and A. Aspect, "A study of atom localization in an optical lattice by analysis of the scattered light," *J. Mod. Opt.* **44**, 1837–1851 (1997).
16. S. Friebe, C. D'Andrea, J. Walz, M. Weitz, and T. W. Hänsch, "CO₂-laser optical lattice with cold rubidium atoms," *Phys. Rev. A* **57**, R20–R23 (1998).
17. R. Scheunemann, F. S. Cataliotti, T. W. Hänsch, and M. Weitz, "An optical lattice with single lattice site optical control for quantum engineering," *J. Opt. B* **2**, 645–650 (2000).
18. S. Hamann, D. Haycock, G. Kiose, D. Pax, I. Deutsch, and P. Jessen, "Resolved-sideband Raman cooling to the ground state of an optical lattice," *Phys. Rev. Lett.* **80**, 4149–4152 (1988).
19. C. Cohen-Tannoudji and D. Guery-Odelin, *Advances in Atomic Physics: An Overview* (World Scientific, 2011), p. 139.
20. T. Takekoshi and R. J. Knize, "CO₂ laser trap for cesium atoms," *Opt. Lett.* **21**, 77–79 (1996).
21. T. Takekoshi, B. M. Patterson, and R. J. Knize, "Observation of optically trapped cold cesium molecules," *Phys. Rev. Lett.* **81**, 5105–5108 (1998).
22. R. Grimm, M. Weidemüller, and Yu. B. Ovchinnikov, "Optical dipole traps for neutral atoms," *Adv. At. Mol. Opt. Phys.* **42**, 95–170 (2000).
23. D. J. Wineland and W. M. Itano, "Laser cooling of atoms," *Phys. Rev. A* **20**, 1521–1540 (1979).